MOLECULAR AND CELLULAR BIOLOGY, Oct. 2007, p. 7302–7314 Vol. 27, No. 20
0270-7306/07/$08.00+0 doi:10.1128/MCB.00758-07

The Forkhead Factor FoxE1 Binds to the Thyroperoxidase Promoter during Thyroid Cell Differentiation and Modifies Compacted Chromatin Structure▽

Isabel Cuesta,[1,2]† Kenneth S. Zaret,[2] and Pilar Santisteban[1]*

Instituto de Investigaciones Biomédicas Alberto Sols, Consejo Superior de Investigaciones Científicas and Universidad Autónoma de Madrid, Madrid 28029, Spain,[1] and Cell and Developmental Biology Program, Fox Chase Cancer Center, 333 Cottman Avenue, Philadelphia, Pennsylvania 19111[2]

Received 30 April 2007/Returned for modification 29 May 2007/Accepted 9 August 2007

The Forkhead box (Fox) transcription factors play diverse roles in differentiation, development, hormone responsiveness, and aging. A pioneer activity of the Forkhead factors in developmental processes has been reported, but how this may apply to other contexts of Forkhead factor regulation remains unexplored. In this study, we address the pioneer activity of the thyroid-specific factor FoxE1 during thyroid differentiation. In response to hormone induction, FoxE1 binds to the compacted chromatin of the inactive thyroperoxidase (TPO) promoter, which coincides with the appearance of strong DNase I hypersensitivity at the FoxE1 binding site. In vitro, FoxE1 can bind to its site even when this is protected by a nucleosome, and it creates a local exposed domain specifically on H1-compacted TPO promoter-containing nucleosome arrays. Furthermore, nuclear factor 1 binds to the TPO promoter simultaneously with FoxE1, and this binding has an additive effect on FoxE1-mediated chromatin structure alteration. On the basis of our findings, we propose that FoxE1 is a pioneer factor whose primary mechanistic role in mediating the hormonal regulation of the TPO gene is to enable other regulatory factors to access the chromatin. The presented model extends the reported pioneer activity of the Forkhead factors to processes involved in hormone-induced differentiation.

In eukaryotes, genetic material is organized inside the cell nuclei into higher-order chromatin structures that play an essential role in regulating the transcription of specific genes at the appropriate time and place by limiting the access of transcription regulators to DNA, among other mechanisms. Many different mechanisms have evolved to overcome the impediment to accessing DNA provided by chromatin structure, such as chromatin remodelling and the modification of enzymes (24, 27, 36, 53). There is increasing evidence that these enzyme complexes are brought to the regulatory regions by certain transcription factors occupying their binding sites (4, 17, 47). Some factors involved in early developmental decisions of cell fates, such as Forkhead box A (FoxA), GATA4 (8), and EBF (32), can bind their target DNA sites within silent chromatin and initiate by themselves chromatin-opening events, defining a new functional class of proteins, the "pioneer" factors.

FoxA factors function as pioneer factors in liver development, since their binding site at the albumin enhancer is occupied in undifferentiated endoderm cells prior to albumin activation (22), they are necessary for albumin transcription and liver specification (29), and they are sufficient to engage and open compacted chromatin in vitro (8, 56). FoxA belongs to the Forkhead family of transcription factors, which are essential for diverse gene regulatory events in differentiation, development, hormone responsiveness, and aging (5, 6, 26, 29). Forkhead factors are characterized by a highly conserved winged helix DNA binding domain, whose structure is similar to the globular domain of the linker histone H5 (10, 42). This similarity has led to the suggestion of an overlapping mechanism of interaction with chromatin structures. Indeed, the Forkhead domain of FoxA1 can bind to nucleosomes even more stably than to free DNA (9) and works in conjunction with a carboxy-terminal histone binding domain to alter chromatin structure (8). However, it is unknown whether the chromatin-opening activity of FoxA proteins is shared by other Forkhead factors.

To address this issue, we have focused on the regulation of thyroid differentiation by the Forkhead factor FoxE1 (formerly called thyroid transcription factor 2 [TTF-2]). FoxE1 regulates the expression of thyroid-specific genes (13, 19, 46), and it is essential for thyroid gland formation (12) and migration (14), being at the center of a regulatory network of transcription factors and cofactors that initiate thyroid differentiation (41). Mutations of the FoxE1 gene cause human syndromes that are associated with thyroid agenesis, among other phenotypes (7, 11). FoxE1 is also necessary for the maintenance of the thyroid differentiated state, because it is essential for the hormonal control of the transcription of thyroid-specific genes, such as the thyroglobulin (Tg) (43) and thyroperoxidase (TPO) (2) genes. TPO gene expression is also regulated by TTF-1 (Nkx2.1), Pax8, and nuclear factor 1 (NF-1). Among these factors, FoxE1 is the main mediator of TPO response to thyroid-stimulating hormone (TSH) and insulin-like growth factor 1 (IGF-1) (2). The expression of FoxE1, as well as its DNA binding and transcriptional activity, is activated by TSH and IGF-1, with the FoxE1 DNA binding site constituting a hor-

* Corresponding author. Mailing address: Instituto de Investigaciones Biomédicas Alberto Sols, Consejo Superior de Investigaciones Científicas and Universidad Autónoma de Madrid, Madrid 28029, Spain. Phone: 34-915854455. Fax: 34-915854401. E-mail: psantisteban@iib.uam.es.

† Present address: Centro Nacional de Biotecnologia, CSIC, Madrid, Spain.

▽ Published ahead of print on 20 August 2007.

mone response element that regulates the specific expression of thyroid genes (40).

For the present paper, we investigated the molecular mechanism of transcription regulation by FoxE1 and its possible role in modulating chromatin structure during the regulation of TPO gene expression by addressing the chromatin structure and transcription factor occupancy of the TPO promoter. We found that during hormonal induction of thyroid cell differentiation, FoxE1 is an initial binding factor to the TPO promoter, prior to gene activation. This binding is coincident with the alteration and opening of TPO promoter chromatin structure, constituting an initial step in the cascade of events that eventually lead to TPO expression. Furthermore, we show in a purified system that FoxE1 can bind and specifically alter the compacted state of the TPO promoter chromatin structure, creating a local open domain.

NF-1 is also an early binding factor during hormonally induced TPO gene activation, and it is present at the TPO promoter simultaneously with FoxE1. FoxE1 and NF-1 are necessary for maximal TPO expression, and they have a synergistic effect on TPO transcription activation that depends on the specific spatial conformation of their binding sites (39). This can be explained by the observation that FoxE1 modification of chromatin structure is enhanced by NF-1 binding to the same nucleosome particle.

MATERIALS AND METHODS

Cell culture and differentiation. PCCl3 cells (20) were grown in Coon's modified Ham's F-12 medium supplemented with 5% donor calf serum and a six-hormone mixture (1 nM TSH, 10 μg/ml insulin, 10 ng/ml somatostatin, 5 μg/ml transferrin, 10 nM hydrocortisone, and 10 ng/ml glycyl-L-histidyl-L-lysine acetate) (complete medium) until they reached 80% confluence. The partially undifferentiated state was induced by maintaining the cells for 8 to 10 days in a medium depleted of TSH and insulin in the presence of 0.2% serum only (basal medium). When indicated, cells were stimulated with 1 nM (0.5 mU/ml) TSH for 2, 10, or 24 h. As a nonthyroid cell control we used a rat hepatoma (H35) cell line (cultured in Dulbecco's modified Eagle medium supplemented with 5% calf serum and 5% fetal serum) and rat embryonic fibroblasts (cultured in Dulbecco's modified Eagle medium supplemented with 15% fetal serum, 1% [vol/vol] sodium pyruvate). The differentiation state was monitored by detection of the mRNA levels of FoxE1, Tg, and TPO at each time point by Northern blot analysis using specific probes.

Chromatin structure analysis. To map the DNase I-hypersensitive sites in the proximal promoter region, nuclei prepared from cells at different stages of differentiation were prewarmed for 45 s and digested at 37°C for 2 min with 0, 0.3, 1.5, 3, 12, or 24 μg/ml of DNase I (Worthington Biochemical Corp.) in a buffer containing 10 mM Tris (pH 7.4), 10 mM NaCl, 3 mM $MgCl_2$, 3 mM β-mercaptoethanol, and 0.5 mM phenylmethylsulfonyl fluoride (PMSF). For nucleosome mapping, PCCl3 cell nuclei were reconstituted in a buffer containing 10 mM Tris (pH 7.4), 50 mM KCl, 15 mM NaCl, 0.5 mM PMSF, 0.15 mM spermine, and 0.5 mM spermidine. After the addition of $CaCl_2$ to a 3 mM final concentration, the samples were prewarmed for 45 s and partially digested with 0, 1.5, 3, 6, or 12 U/ml of micrococcal nuclease (MNase; Worthington Biochemical Corp.) for 4 min at 37°C. Extracted genomic DNA was digested with EcoRI and analyzed on Southern blots with probes corresponding to the −2468- to −3174-nucleotide (nt) fragment (DraIII-PstI) of the rat TPO promoter region. Free DNA samples were obtained by digestion of 80 to 100 μg of untreated genomic DNA with 0, 0.3, or 1.5 U/ml MNase and 0, 1.5, or 6 μg/ml DNase I for 1 min at 23°C. G and A→C sequencing reactions were done as described previously (34).

In situ methylation of PCCl3 DNA. PCCl3 cells under the different experimental conditions were treated with a medium containing 0.1% (vol/vol) dimethyl sulfate (DMS) for 2 min 30 s at 23°C, and the methylation reaction was stopped by several washes with phosphate-buffered saline and extraction of the cell nuclei. Genomic DNA was extracted and treated with 10% (vol/vol) piperidine for 10 min at 90°C. Piperidine was eliminated by three successive lyophilization steps of 2 h each. DNA was finally diluted in H_2O at a known concentration and stored at −20°C.

Analysis of chromatin by LM-PCR. Ligation-mediated PCR (LM-PCR) was performed on DNase I- and DMS-piperidine-cleaved DNA essentially as described previously (38). One to 3 μg genomic DNA was used for the initial primer (TPO1 oligo; see below) extension using T7 Sequenase DNA polymerase v.2.0 (U.S.B). Double-stranded linker oligonucleotide ligation was done at 16°C for 16 h with T4 DNA ligase (Boehringer). DNA fragments were amplified by a standard PCR with long linker and TPO2 (see below) oligos for 20 cycles of 1 min at 96°C, 2 min at 58°C, and 3 min at 72°C. To visualize them on a gel, the resulting DNA fragments were then amplified with a third radiolabeled oligo, TPO3 (see below), by one cycle of 2 min at 96°C, 2 min at 63°C, and 10 min at 72°C. After the PCRs were stopped, DNA was purified and analyzed on 6% acrylamide and 7 M urea sequencing gels. Gels were dried, DNA fragments were visualized by autoradiography, and the autoradiographs were scanned. The intensities of individual lanes were quantified by scanner densitometry and normalized to a band outside the footprinted area (indicated in the figures). The results are presented as percentages of enhancement and protection by dividing the normalized intensities of the particular bands in cell samples by the normalized band in the protein-free sample. Plots of the DNase I digestion pattern were obtained by exposing the gels to a FUJI phosphorimager and analyzed using the Image Gauge program. MNase-digested DNA samples were first phosphorylated with T4 polynucleotide kinase (New England Biolabs) in the presence of 0.1 mM ATP for 1 h. Three micrograms of MNase samples was amplified by LM-PCR from the ligation step, omitting the first extension step. Sequences of the primers and terminal nucleotide numbers were as follows: for TPO1, (−257) ATAAGA GAAACTCCCAGGAACC (−236); for TPO2, (−242) AGGAACCTATGTGG GTGACC (−223); and for TPO3, (−231) TGGGTGACCCTAGCTAAGACAC (−210).

ChIP. After treatment with 1% formaldehyde for 10 min at 37°C, the cross-linking reaction was stopped by the addition of glycine to a final concentration of 125 mM, and the cells were collected in permeabilization buffer [5 mM piperazine-*N*,*N*′-bis(2-ethanesulfonic acid) (PIPES) (pH 8.0), 85 mM KCl, 0.5% (vol/vol) NP-40, 1 mM PMSF, 5 mM Na butyrate, and a protease inhibitor cocktail (Roche Diagnostics). After centrifugation, cells were resuspended in lysis buffer (50 mM Tris [pH 8.1], 10 mM EDTA, 1% [wt/vol] sodium dodecyl sulfate [SDS], and the same protease inhibitor cocktail as indicated above), and the chromatin was fractionated by ultrasound sonication. Chromatin immunoprecipitation (ChIP) was performed with 100 μg of Sepharose A-precleared chromatin in 0.01% (wt/vol) SDS, 1.1% (vol/vol) Triton X-100, 1.2 mM EDTA, 16.7 mM Tris (pH 8), 167 mM NaCl with 1 μg of affinity-purified antiserum. Antibody-bound chromatin was brought down with protein A-Sepharose beads followed by extensive washing with increasing NaCl concentrations and elution with 1% (wt/vol) SDS, 100 mM $NaHCO_3$ (as described in reference 18). After reversing the cross-linking in 200 mM NaCl at 65°C, the DNA was purified and analyzed by PCR. The antibodies used in this study were anti-rFoxE1 (kind gift of R. Di Lauro, BIOGEM, Ariano Irpino, Avellino, Italy) and anti-NF-1 (Santa Cruz Biotechnology). The immunoprecipitated DNA was analyzed by PCR using specific primers that amplify 288 nt of TPO promoter (for TPO-F, ATAAGAG AAACTCCCAGGAACC; for TPO-R, ACTTCAGAAATGTGAATCTCAA) and 254 nt of rat β-actin exon 3 (for actin-F, AACACCCCAGCCATGTAC; for actin-R, ATGTCACGCACGATTTCC).

Nucleosome array reconstitution. TPO promoter fragments were amplified by PCR using the primers TPO-P1 [5′-TTT GCT AGC$^{(-444)}$CAT CTT GTA GAC AGG AC$^{(-428)}$-3′], TPO-P3 [5′-TTT GCT AGC$^{(-487)}$TAG GTT GGT ATC CCT GG$^{(-471)}$-3′], TPO-P5 [5′-AAA GCT AGC$^{(-401)}$ACA AGA GGC ATC TGG AC$^{(-385)}$-3′], TPO-Pa [5′-TTT GTT GAC$^{(+57)}$GAG CTG GGT GTG TTC TT$^{(+42)}$-3′], and TPO-Pb [5′-TTT TGA TCA$^{(+47)}$GTT CTT TGT GGC CTT AA$^{(+31)}$-3′]. The PCR products were cut with NheI and BclI and subcloned into NheI-BclI-digested pN2N1P (8) to create TPO nucleosome arrays. The TPO-5b array contains the TPO promoter from position +47 to position −401 fused to the Neo reporter gene and inserted between 10 tandem repeats of the sea urchin 5S ribosomal DNA (rDNA) sequence. Preparation of the end-labeled ^{32}P probe DNA and nucleosome array reconstitution were carried out as described previously (8).

Transcription factor purification and characterization. The pET28b-FoxE1 protein expression plasmid was constructed from pBS-FoxE1 (55). An NdeI site was introduced by site-directed mutagenesis (Stratagene), generating the construct pBS-FoxE1-NdeI. The NdeI-BamHI fragment of pBS-FoxE1-NdeI was cloned into pET28b (Novagen), generating the construct pET28b-FoxE1, which encodes rat FoxE1 fused to a six-histidine tag. His-tagged rat FoxE1 and mouse FoxA1 were purified from *Escherichia coli* and analyzed by gel electrophoresis and Western blotting using the anti-rFoxE1 antibody. An electrophoretic mo-

bility shift assay was carried out as described previously (57) with ^{32}P-labeled double-stranded oligo Z derived from the TPO promoter (19) and 1.3 pmol of purified factors. Human NF-1 was a kind gift from N. Tanese (NYU, NY) to K. S. Zaret.

Binding reactions and enzymatic analysis. Binding reactions were carried out by incubating 1 nM nucleosome arrays (13 nM nucleosomes) with 10 to 13 nM H1 (Calbiochem) for 1 h at 23°C in 20 mM HEPES (pH 7.5), 50 mM KCl, 5% (vol/vol) glycerol, 2 mM dithiothreitol, and 100 μg/ml bovine serum albumin; next, the indicated transcription factors were added to a final concentration of 20 nM, and incubation was continued for 2 h at 23°C. DNase I and restriction enzyme digestion were carried out and analyzed essentially as described previously (8). For the enzyme digestion experiments, autoradiographs were scanned and the intensities of individual bands in the lanes were quantified by scanner densitometry. To calculate the percentages of cut product, the bands corresponding to the 45-min time point were used, and means and ranges were calculated.

RESULTS

Chromatin structure of the active and inactive TPO minimal promoters in differentiated thyroid cells. TPO gene expression is controlled by a minimal promoter necessary and sufficient to confer tissue specificity, which contains the binding sites for all known transcription factors that regulate it (Fig. 1A). We have characterized the chromatin structure of the active and inactive TPO promoters. The active state is present in the PCCl3 thyroid cells cultured in a hormone-supplemented medium, where the cells are fully differentiated and express the thyroid marker Tg, TPO, and FoxE1 genes (Fig. 1B, lane 1). The inactive state is obtained by culturing PCCl3 cells in a medium depleted of TSH, insulin, and serum. In these conditions, the cells obtain a quiescent, partially undifferentiated state, where Tg, TPO, and FoxE1 mRNAs are no longer detected (Fig. 1B, lane 2).

The nucleosomal organization of the TPO promoter in both active and inactive states was studied by treatment of PCCl3 cell nuclei with MNase. The digested chromatin fragments were analyzed by indirect end labeling with a probe (DraIII-PstI) that hybridizes upstream of the minimal promoter (Fig. 1E). The TPO minimal promoter, which is located between the SacI and BstXI restriction sites (Fig. 1C, lane 9), has in the active state a structure that is more open and susceptible to MNase digestion than the flanking sequences (lanes 5 to 8). The cleavage pattern is distinct from that obtained with free DNA (Fig. 1C, lanes 2 and 3). The three MNase-hypersensitive sites indicate the presence of three positioned nucleosome-like particles (Fig. 1C, lanes 5 to 8, and E). Particle A is located over the transcription start site, while particles B and C are positioned over the minimal promoter, with the BstXI and SacI sites in apparent linker regions (Fig. 1E). The inactive state of the TPO promoter presents the same MNase pattern as the active promoter, but overall it is more resistant to the same concentration range of MNase, indicating a more compacted chromatin structure (Fig. 1C, lanes 10 to 13). In the nonthyroid cell line H35, the structure of the silent TPO minimal promoter also remains resistant to MNase (Fig. 1C, lanes 16 to 18).

To further characterize the TPO promoter, we addressed the occupancy of its regulatory elements by treating PCCl3 cells in the active and inactive states with DNase I (31). A unique DNase I-hypersensitive region appears in the active state (Fig. 1D, lanes 5 and 6) and is located over the sequences protected by particle B described above (compare panels C and D), indicating that this nucleosome-like particle becomes more exposed during TPO expression (Fig. 1E).

To accurately map the position of the nucleosome-like particle B, we analyzed the MNase cleavage sites at the nucleotide level by use of a modified LM-PCR technique (35) with a primer set that anneals to the 5′ end of the minimal promoter. The active promoter presents two clusters of MNase cleavage sites (Fig. 2A, lanes 3 to 6), in comparison to what is seen for MNase cleavage of protein-free DNA (lanes 1 and 2). These sites are located at both sides of a more protected region defining the preferential translational position of particle B, in agreement with the low-resolution mapping experiment (Fig. 1C). Particle B therefore spans about 150 bp and comprises the binding sequences of all known transcription factors that regulate TPO gene expression (Fig. 1A), leaving the BstXI site in the apparent linker DNA (Fig. 2A, right). The 3′-TTF-1/Pax8 and 5′-TTF-1 binding sites are near the edges of particle B, whereas the FoxE1 site is located near the middle. The MNase cleavage, which defines particle B, is weaker in the inactive TPO promoter and completely absent in nonthyroid cells (Fig. 2A, lanes 7 to 10 and 11 to 14, respectively), which also agrees with the results from the low-resolution mapping.

Specific binding of the regulatory transcription factors in the active TPO promoter. To study the in vivo occupancy of the transcription factor binding sites in the active and inactive TPO promoters, we performed DMS and DNase I genomic footprinting. The DMS footprint of the active and inactive promoters reveals a change in the accessibility of the FoxE1 site nucleotides. In the active state, methylation was significantly reduced (27%) in the 3′ guanosine, while it was enhanced (210%) in the one next to it (Fig. 2B, lane 1) compared with what was seen for nonexpressing cells and protein-free DNA (Fig. 2B, lanes 2 and 3, respectively). This pattern seems to indicate that the FoxE1 biding site is occupied only in the active TPO promoter (see below). The changes in the methylation pattern of the binding sites for the other transcription factors also indicate different occupancies in the active and inactive promoters (Fig. 2B, lanes 1 and 2; compare percentages).

High-resolution DNase I footprinting analysis of the active TPO promoter presents a strong and characteristic enhancement of local DNase I cleavages in the FoxE1 binding site compared to what is seen for the inactive state (Fig. 2C, compare lanes 1 and 2 with lanes 3 and 4), supporting FoxE1 site occupancy at the active promoter as described above. The strong protection against DNase I digestion at the NF-1 and central TTF-1 sites and the general alteration of the DNase I pattern over the 3′-TTF-1/Pax8 sites led us to think of a general occupancy of the binding sites in the active TPO promoter. Interestingly, TTF-1, Pax8, and NF-1 are expressed in cells maintained in the inactive state, while TPO or FoxE1 are not (39), but their binding sites in the TPO promoter seem to become occupied only after induction of the active cell state, when TPO and FoxE1 are expressed.

Recruitment of the transcription factors during the induction of TPO expression. TSH treatment of quiescent PCCl3 cells strongly activates the expression of the TPO, Tg, and FoxE1 genes; maximum mRNA levels are reached after 24 h of hormonal induction (40, 58), although these levels are not as high as in the active state, where the cells receive more stim-

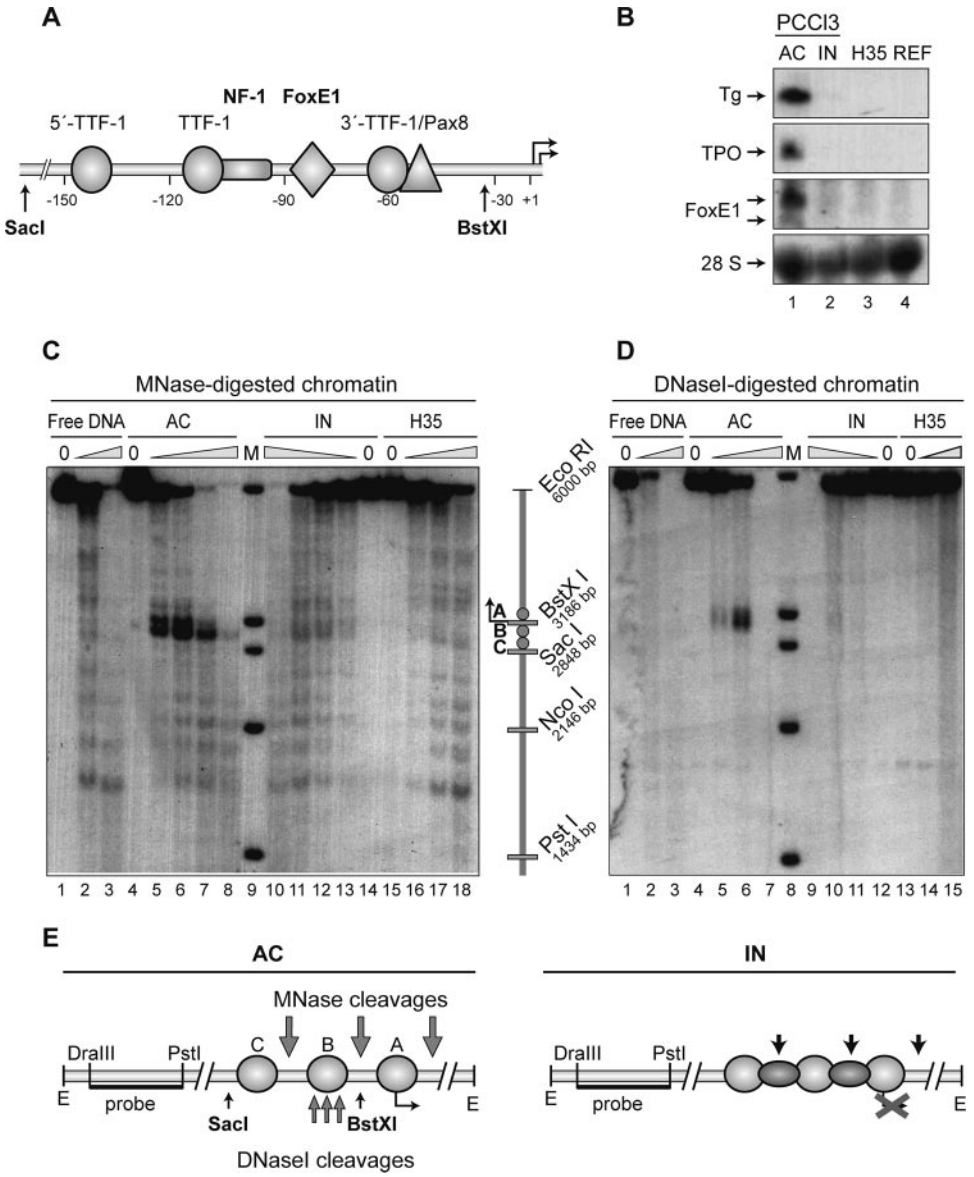

FIG. 1. Analysis of the chromatin structure of the active and inactive TPO minimal promoters. (A) Schematic representation of the minimal TPO promoter between positions −150 and +1, showing the binding sites of the known transcription factors that regulate its expression. Arrows indicate the two transcription start sites. (B) Representative Northern blot of total RNA from PCCl3 cells maintained under differentiated (active [AC]) or quiescent (inactive [IN]) conditions as well as from the nonthyroid cell type H35 and rat embryonic fibroblasts hybridized with specific probes for the thyroid-specific Tg, TPO, and FoxE1 genes. The 28S rRNA probe was used as a loading control. (C and D) Nuclei from AC or IN PCCl3 cells and H35 cells were digested with increasing concentrations of MNase (C) and DNase I (D), and the resulting fragments were analyzed by indirect end labeling of the EcoRI-digested genomic DNA with the DraIII-PstI probe shown in panel E. As a control, protein-free DNA was also digested with MNase and DNase I. As a marker (M), protein-free DNA digested with PstI, NcoI, SacI, and BstXI was used. The sizes of the resulting fragments are indicated. (E) Schematic of the AC and IN TPO promoter chromatin structures, summarizing MNase and DNase I cleavage sites. The positions of the nucleosome-like particles are indicated as closed circles and are designated A, B, and C. Unknown factors that protect DNA from endonuclease digestion are indicated by small dark ellipses. The TPO expression state is indicated by an arrow (AC) from particle A at position +1 (the transcription start site) or by a cross (IN).

ulation. To have a simple and well-controlled system, we studied transcription factor recruitment to the TPO promoter during gene activation by treating quiescent thyroid cells with TSH for various times (Fig. 3A). FoxE1 mRNA was rapidly detectable after 2 h of TSH induction (Fig. 3B, lane 3), and its expression was maintained at 10 and 24 h (lanes 4 and 5). The expression of the thyroid-specific Tg and TPO genes was more delayed, being detected after 10 h and reaching maximum levels at 24 h of TSH induction (Fig. 3B, lanes 3 to 5).

The accessibility of the TPO promoter and the occupancy of its *cis*-regulatory elements were determined by assessing DNase I hypersensitivity at various times of TSH induction (Fig. 3C and D). As reported above, the TPO minimal promoter is DNase I hypersensitive in the active state when the

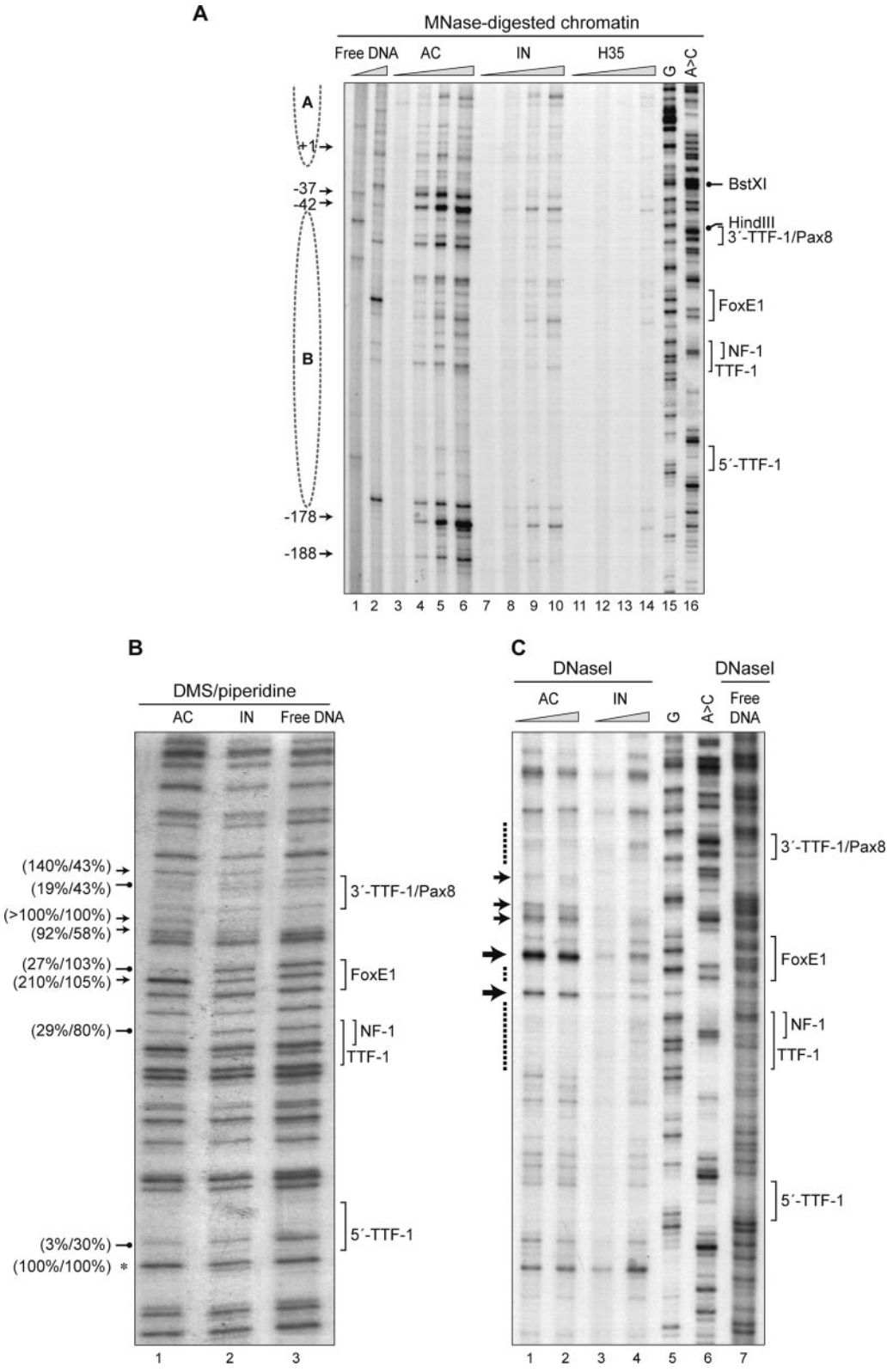

FIG. 2. Analysis of transcription factor binding site occupancy in the active (AC) or inactive (IN) TPO promoter. (A) Nuclei from AC or IN PCCl3 cells and H35 cells and protein-free DNA were digested with increasing concentrations of MNase, and the DNA fragments were analyzed by modified LM-PCR and resolved on a sequencing gel. Maxam and Gilbert sequencing reactions for G and A>C were used to identify DNA sequences (34). The strong specific MNase cleavage sites and the region protected by particle B are indicated on the left side of the panel, as is the transcription start site. The relative positions of the transcription factor binding sites and the restriction enzyme recognition sequences are indicated on the right. (B and C) In vivo footprinting analysis of the TPO promoter by DMS (B) and DNase I (C) protection in AC or IN PCCl3 cells. The bottom strands of the DNA

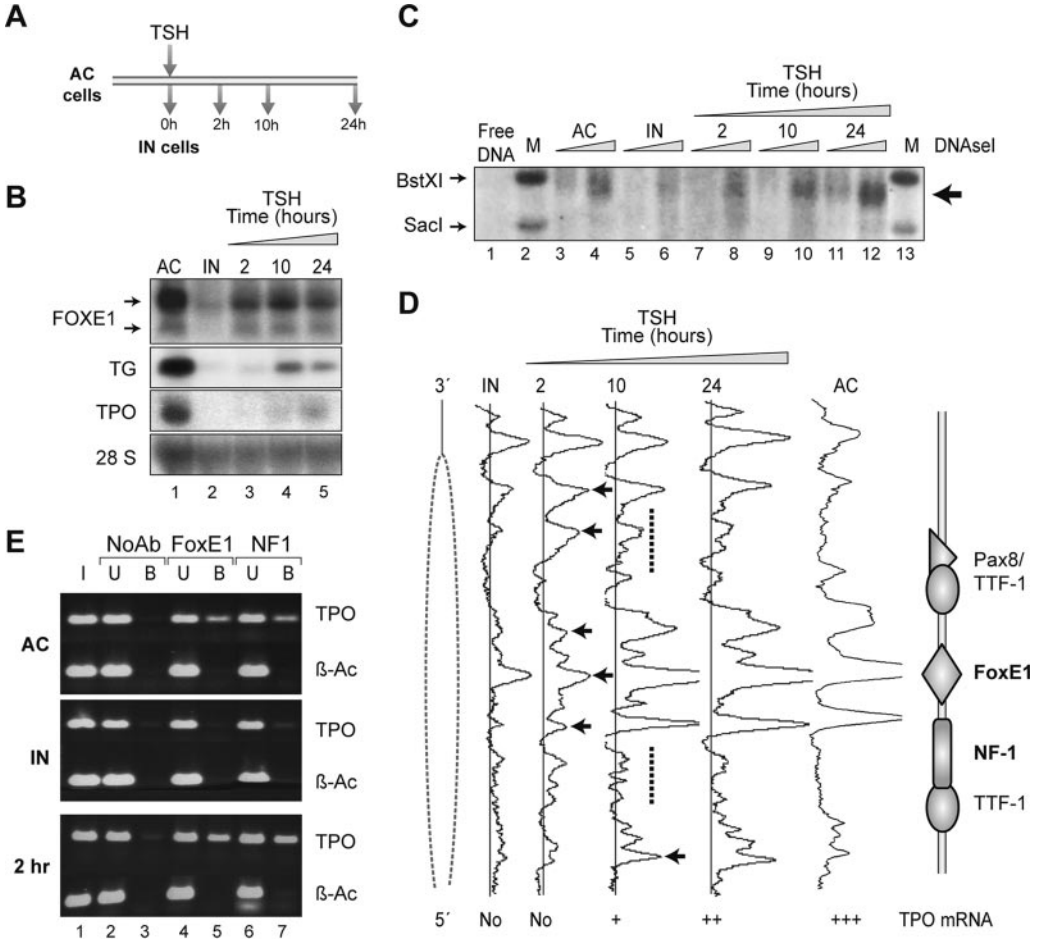

FIG. 3. Order of transcription factor binding site occupancy during TPO gene activation. (A) Experimental design to study the order of events that take place prior to TPO gene expression. Differentiated PCCl3 cells (active [AC]) were maintained in hormone-deprived media for several days until they reached the quiescent state (inactive [IN]). TPO expression was induced by treatment with TSH for 2, 10, and 24 h. (B) mRNA levels of the thyroid-specific Tg, TPO, and FoxE1 genes were detected by Northern blotting using specific probes. The 28S rRNA probe was used as the loading control. (C and D) Analysis of the DNase I-hypersensitive sites in the TPO promoter: nuclei of AC, IN, and TSH-induced cells were digested with increasing concentrations of DNase I and analyzed by indirect end labeling (C) or LM-PCR (D). (C) Protein-free DNA digested with BstXI and SacI was used as a marker to localize the minimal TPO promoter. The arrow indicates the DNase I-hypersensitive region. (D) Plots of the DNase I cleavage patterns resolved at the nucleotide level. The relative positions of transcription factor binding sites inside particle B (dashed outline at left) are indicated. Dotted lines indicate DNase I-protected sequences, and arrows point at the DNase I-hypersensitive sites as they appear. TPO mRNA levels of each experimental condition are shown under each plot. (E) ChIP assay. Soluble chromatin from cells in the AC or IN state or after 2 h of TSH induction was immunoprecipitated with FoxE1 or NF-1 antibodies. A control with no antibody (NoAb) was included. The DNA in the unbound (U) and bound (B) fractions and input DNA (I) was PCR amplified with TPO promoter-specific primers. β-Actin primers (β-Ac) were used as the negative control.

TPO gene is expressed (Fig. 3C, lanes 3 and 4), while it is more protected in the inactive state (lanes 5 and 6). TSH treatment provokes the appearance of hypersensitivity in the promoter, which is detectable within the first 2 hours and increases after longer times of induction (Fig. 3C, lanes 7 to 12). The DNase I-hypersensitive sites were mapped at the nucleotide level (data not shown), and the profiles were plotted (Fig. 3D). As expected, the inactive TPO promoter is protected from DNase

fragments were amplified by LM-PCR. Protein-free DNA was used as the control. In panel B, the average percentages of methylation at particular guanosines in AC or IN cells, compared with what was seen for protein-free DNA, are given in parentheses. ">100%/100%" indicates a very strong hypersensitivity in the AC cell sample and a similar value in the IN cell sample, in comparison to what was seen for the corresponding band seen for protein-free DNA; this latter band could not be quantified accurately due to its low intensity. Bands outside the footprinted area used for normalization are indicated by an asterisk. In panel C, protected and hypersensitive nucleotides are indicated by dots/dotted lines and arrows, respectively. The positions of the transcription factor binding sites were localized by Maxam and Gilbert sequencing reactions of G and A>C and are indicated on the right of the gel. For panel B, methylation enhancements are indicated by arrows, while reductions are indicated by dashes. For panel C, large arrows indicate the strong and characteristic enhancement of local DNase I cleavages in the FoxE1 binding site for the AC TPO promoter compared to what is seen for the IN state.

I digestion, showing a nearly flat DNase I profile (Fig. 3D, IN profile). After only 2 h of TSH induction, the hypersensitivity appearing over the TPO promoter coincides with FoxE1 binding site occupancy (Fig. 3D, 2-h profile) and precedes a significant increase in TPO mRNA accumulation (Fig. 3B, lane 3). The DNase I profiles of the promoter at 10 and 24 h of TSH induction reveal further changes in the nucleotide accessibility of the factor binding sites, with the appearance of more protected and more exposed nucleotides. At 24 h, the profile is much like that of the active promoter (compare 24-h profile and AC profile).

As FoxE1 is already expressed after 2 h of TSH induction (Fig. 3B, lane 3), we wanted to investigate if FoxE1 binding is causing the DNase I-hypersensitive sites appearing after 2 h over its binding site by use of a ChIP assay (Fig. 3E). FoxE1 is bound to the active TPO promoter, and this binding is no longer detectable in the inactive state (Fig. 3E, lane 5), as expected from the lack of FoxE1 expression in quiescent cells (Fig. 3B). After 2 h of TSH induction, newly expressed FoxE1 is already bound to the TPO promoter (Fig. 3E, bottom, lane 5), probably causing some of the DNase I-hypersensitive sites seen at this time point over its binding site (Fig. 3D).

One of the DNase I-hypersensitive sites found after 2 h of TSH induction is located close to the NF-1 binding site. ChIP with NF-1 antibodies revealed that NF-1 is bound to the TPO promoter at this time, together with FoxE1 (Fig. 3E, lane 7). Interestingly, NF-1 is not bound to the inactive TPO promoter in quiescent cells (Fig. 3, middle, compare lanes 3 and 7), even though NF-1 is expressed in these cells, unlike FoxE1 (39). The specificity of FoxE1 and NF-1 binding to the TPO promoter sequence was confirmed by using as a negative control a PCR-amplified region of the β-actin gene corresponding to exon 3 that does not contain any of the binding sites for these transcription factors.

Reconstitution of nucleosomal arrays containing the TPO promoter. To study the molecular mechanism of TPO gene activation by FoxE1 in vivo, we sought to mimic the process in vitro with the TPO promoter sequence inserted into a phased nucleosome array (8, 28, 49, 50). Four different TPO nucleosome array constructs were created by placing five tandem repeats of the 5S rDNA nucleosome-positioning sequence (45) at both ends of various TPO minimal promoter fragments. These TPO fragments contain nearly identical sequences, but they differ in size and in the relative position of the sequences protected by the nucleosome-like particles described in the in vivo mapping (Fig. 1C and E and 2A). The nucleosome arrays were created by PCR with different primers that anneal upstream (primers 1, 3, and 5) and downstream (primers a and b) of the TPO minimal promoter (schematically shown in Fig. 4A). DNase I and EcoRI digestion assays were performed to characterize the nucleosome arrays after the assembly process in order to assess the integrity and level of histone deposition (Fig. 4B to D). The nucleosome arrays were assembled using two different DNA-to-histone ratios, and the level of saturation was determined by EcoRI digestion (Fig. 4B). The amount of free DNA released in the EcoRI assay shows that the 1:1.2 arrays (lane 2) are subsaturated, while the 1:1.4 arrays (lane 3) are already saturated. The DNase I cleavage pattern (Fig. 4C, lanes 2 and 3) revealed the deposition of 10 evenly spaced nucleosomes over the 5S rDNA sequences and of 2 others over the TPO promoter; we called these sites B and C, as they are positioned over the same sequences relative to the BstXI and SacI restriction sites as the in vivo B and C particles (compare Fig. 4C and 1C). This positioning is independent of the cloning site of the TPO promoter in the array, because after coincubation of the DNA and histones alone, the nucleosomes B and C become localized over the same sequences in all the different TPO arrays (Fig. 4D, lanes 1b, 3b, 5b, and 1a), and only the length of linker DNA flanking particles A′ and C varies. The DNase I-hypersensitive region located between particle B and the first repeat of 5S is composed of a mix of TPO promoter and NEO gene sequences (Fig. 4A). We have named this sequence A′, but although it is long enough to contain a nucleosome particle, we cannot conclude from the present experiments whether it is an exposed/unstable nucleosome or a nucleosome-free region. Thus, our nucleosome arrays constitute an in vitro system that resembles very much the in vivo situation; we chose the TPO-5b array for further analyses, as it is more homogeneous in terms of linker DNA length (Fig. 4C and D).

To mimic the compacted chromatin/nuclease-resistant state of the TPO promoter present in the inactive cells (Fig. 1C and D), we incubated the TPO-5b nucleosome arrays with the linker histone H1 (52). H1 binding caused a marked change in the conformation of the arrays to a nuclease-resistant state, as seen by the inhibition of DNase I sensitivity over a range of enzyme activities that readily digested H1-free arrays (Fig. 4C, compare lanes 2 and 3 with lanes 4 and 5).

FoxE1 opens the H1-compacted chromatin structure of TPO nucleosome arrays. To understand better the role of FoxE1 in the regulation of TPO promoter chromatin structure during gene activation, we investigated the ability of FoxE1 to engage and modify chromatin structure. As a positive control for these activities, we chose the Forkhead factor FoxA1, which binds to the FoxE1 site of the TPO promoter (44) and whose modifier activity of compacted chromatin structure has been reported for another regulatory element (8). Recombinant FoxE1 and FoxA1 were purified from bacteria, and both were able to bind with equal affinities to an oligo containing the FoxE1 binding site and to the TPO nucleosome arrays (data not shown). FoxE1 and FoxA1 were tested on extended (H1-free) and compacted (H1-containing) TPO-5b arrays. The binding of these two factors to the extended TPO-5b arrays did not markedly alter the DNase I hypersensitivity pattern (Fig. 5A, lanes 5 to 8), consistent with the reported FoxA1 activity. By contrast, FoxE1 binding to H1-compacted nucleosome arrays induced a broad DNase I hypersensitivity over nucleosome B, which contains its binding site (Fig. 5B, lanes 6 and 7). This alteration is also produced when using saturated arrays (Fig. 5B, lanes 12 and 13), whose structure is more compacted and resistant to DNase I digestion, indicating that chromatin opening by FoxE1 is not an artifact of a lower nucleosome density over its binding site. More specifically, the overall hypersensitivity is formed by two discrete hypersensitive sites: one at the FoxE1 binding site and the other at the 3′ end of nucleosome B (Fig. 5C, lanes 3 and 4 and schematic). This effect is probably caused by FoxE1-specific binding and not by sequestering histone H1 through unspecific interactions or other events of this nature caused by purified factors in general, because it is discrete and located only over the region that contains the FoxE1

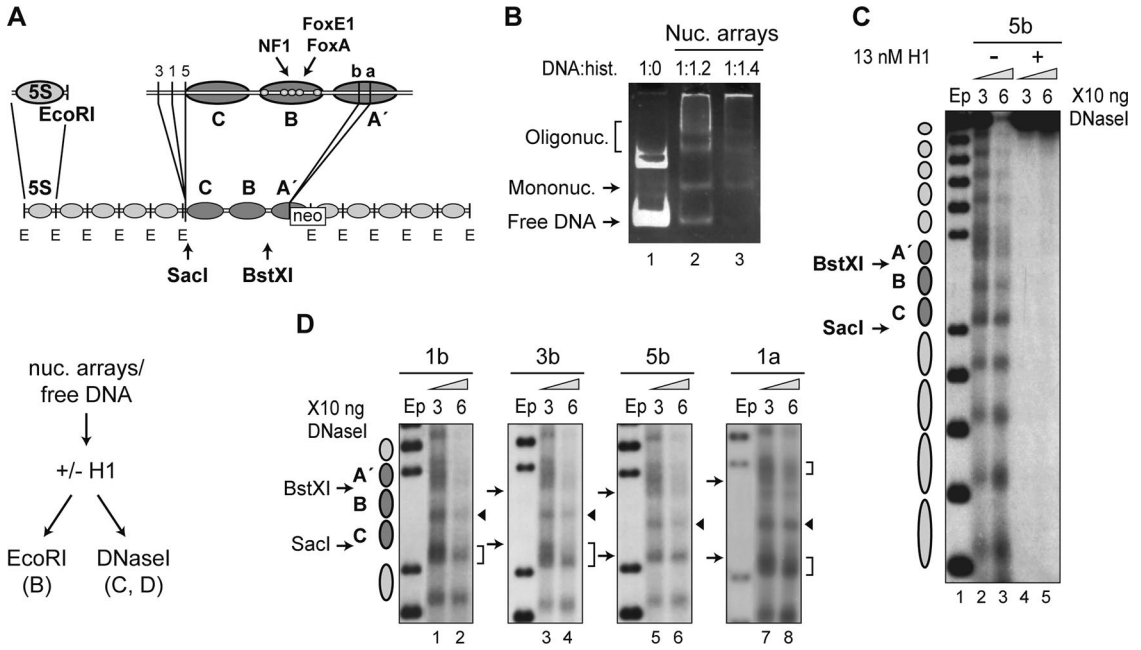

FIG. 4. The TPO minimal promoter containing nucleosome arrays as an in vitro chromatin system. (A) Schematic of the TPO promoter fragments inserted in the final DNA probe used to generate TPO nucleosome arrays. The numbers 1, 3, and 5 indicate the annealing positions of the 5′ primers, whereas the letters a and b indicate the 3′ primers used to obtain the inserted fragments by PCR. Dark ellipses indicate the positions of the nucleosome-like particles (C, B, and A) over the TPO promoter as mapped in vivo (Fig. 1 and 2). The transcription factor binding sites are indicated as small circles inside particle B (ellipse labeled B). The light gray ellipses indicate the positions of the 10 repeats of 5S rDNA nucleosome-positioning sequences. The integrity of nucleosome arrays was assessed by EcoRI (B) or by DNase I (C and D) digestion. (B) Partial EcoRI digestion of the TPO-5b nucleosome arrays to assess the saturation level of nucleosome deposition. The two different DNA-to-histone (DNA:hist.) ratios used to assemble the nucleosome (nuc.) arrays are indicated above the gel. Free DNA was used as a control. The different products are indicated on the left. (C) Partial DNase I digestion of the extended (−) and H1-compacted (+) TPO-5b (5b) nucleosome arrays. The 5S positions revealed by partial EcoRI digestion (Ep) are indicated on the left by light grey ellipses. Dark ellipses indicate the positions of the TPO particles A′, B, and C. DNase I concentrations are shown above the gel. (D) Partial DNase I digestion of TPO nucleosome arrays, in the extended conformation, containing different fragments of TPO promoter; the primers used to obtain each of the fragments are indicated above the panels. DNase I concentrations are shown above the gels. Partial EcoRI digestion of free DNA (Ep) was used as an internal marker of the 5S repeat positions. The linker DNA between particles B and C is indicated by arrowheads on the right of the panels; linker DNA between 5S and TPO promoter sequences is indicated by brackets. BstXI and SacI fragments were used as markers for the position of the minimal TPO promoter, and their relative positions on the gel are indicated by arrows on the left of the panels.

binding site. Other supporting evidence is that FoxA1, which alters chromatin structure in a specific manner as demonstrated by using negative control proteins (8), can bind to the FoxE1 sites (44) and modify the structure of H1-compacted TPO arrays, causing the same pattern of DNase I hypersensitivities, although with higher intensity (Fig. 5C, compare lanes 3 and 4 with lanes 5 and 6). Thus, these results indicate that FoxE1, as reported for FoxA1, can act on compacted chromatin structures and modify them during transcriptional control.

At the early stages of TPO activation, NF-1 is bound together with FoxE1 to the TPO promoter (Fig. 3E), so we also investigated the possible effects of NF-1 on the TPO nucleosomal array structure. Purified NF-1 protein induced a distinct hypersensitive site on extended arrays over the B nucleosome (Fig. 5A, lanes 9 and 10), as well as in histone H1-compacted arrays (Fig. 5C, lanes 7 and 8 and schematic). Although previous reports have failed to see NF-1 binding to compacted nucleosome arrays (8, 48), we suggest that the positive results in our system may be due to an optimal positioning of the NF-1 target sequence on the nucleosomes.

The simultaneous binding of FoxE1 and NF-1 to the TPO promoter has been demonstrated by in vitro footprinting (19, 39). That the same situation occurs in living cells has been confirmed by in vivo footprinting, which showed the same protections over the FoxE1 and NF-1 binding sites as observed in vitro (see above). Therefore, to further mimic the in vivo situation, we analyzed the effects of the simultaneous binding of FoxE1 and NF-1 to the nucleosome B structure. Interestingly, both factors together induced DNase I hypersensitivities at the same sites as each factor alone (Fig. 6A, lanes 5 and 6), suggesting an additive effect on chromatin structure alteration.

To assess chromatin opening in a different way, we employed a restriction enzyme accessibility assay at three different sites, BstXI, HindIII, and SacI (Fig. 6B). Compaction of the nucleosome arrays with histone H1 completely or partially occluded HindIII (from 44% to 10% of cut molecules compared to what was seen for noncompacted arrays) and BstXI (from 57% to 3%) restriction sites, respectively (Fig. 6B, lanes 1 to 4); these sites are located within the sequence protected by nucleosome B for HindIII or at its 3′ linker region for BstXI (Fig. 2A, schematic). The distant SacI site, which is located in the linker sequence between the 5S rDNA nucleosomes and nucleosome C, presents a weaker protection (from 37% to 17%). FoxE1

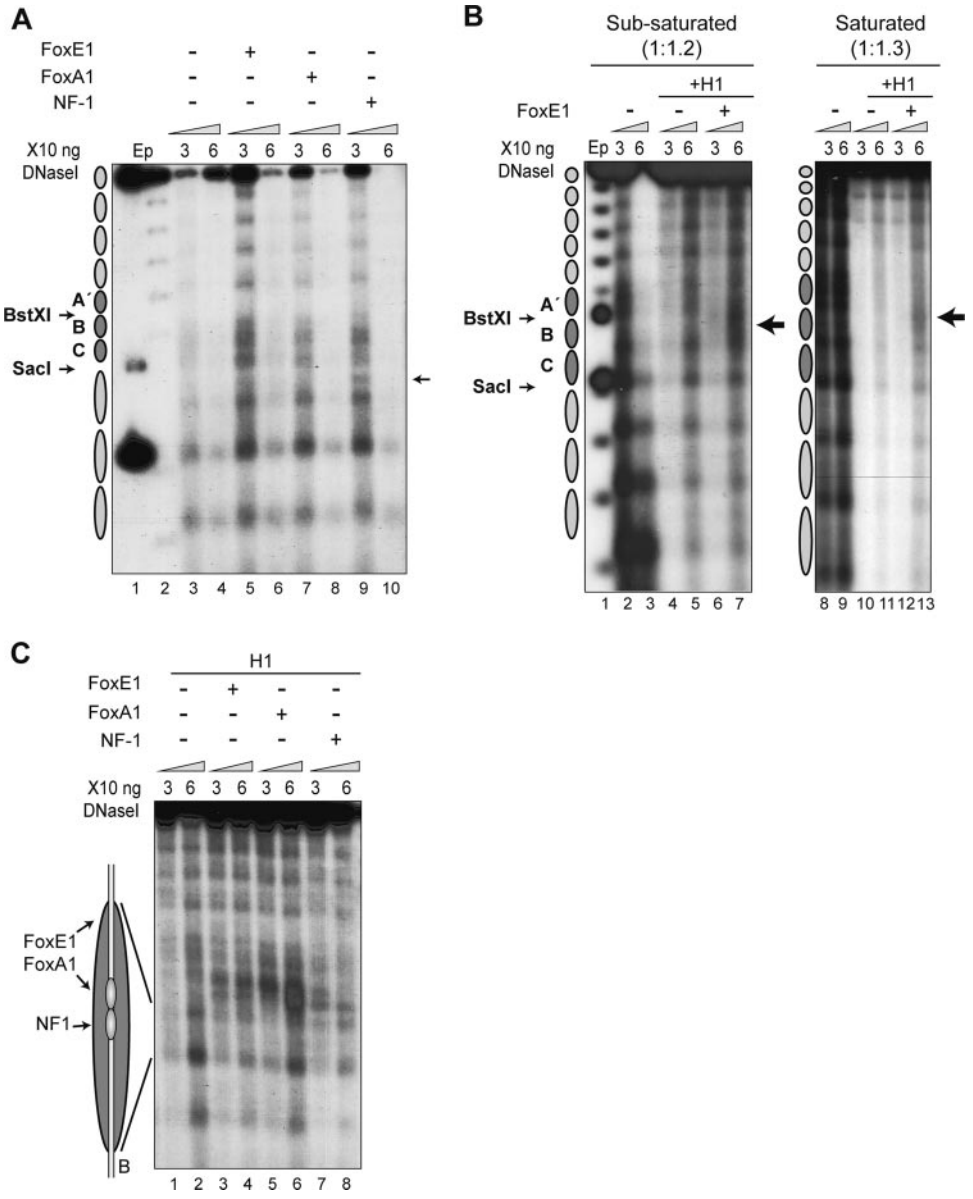

FIG. 5. Modulation of the extended and compacted chromatin structure of the TPO promoter by FoxE1, FoxA1, and NF-1. (A to C) Partial DNase I digestion of the extended and H1-compacted TPO-5b nucleosome arrays incubated with the indicated transcription factors. The positions of the nucleosomes are represented as ellipses (TPO sequences, dark; 5S rDNA sequences, light) to the left of the gels. DNase I concentrations are shown above the gels. Partial EcoRI digestion of free DNA (Ep) was used as an internal marker of the 5S repeat positions. BstXI and SacI fragments were used as internal markers for the position of the TPO minimal promoter. (A) TPO nucleosome arrays in the extended conformation. (B) Subsaturated and saturated TPO nucleosome arrays. The two different DNA-to-histone ratios used to assemble the nucleosome arrays are indicated in parentheses above the gels. Extended and H1-compacted arrays were obtained from the two histone saturation conditions. The large arrows indicate the DNase I-hypersensitive region. (C) TPO nucleosome arrays in the H1-compacted conformation. On the left is a scheme indicating the positions of transcription factor binding sites as lighter ellipses inside particle B.

binding to the compacted arrays enhanced the accessibility of the BstX1 site, but it had no effect on the HindIII site (Fig. 6B, lanes 5 and 6). By contrast, NF-1 binding enhances the accessibility of the HindIII site without altering the accessibility of the BstXI site (Fig. 6B, lanes 7 and 8). FoxE1 and NF-1 had small enhancing and inhibiting effects, respectively, on SacI site accessibility. These results are consistent with the DNase I hypersensitivity assay on TPO arrays, where FoxE1 binding created two exposed regions, one of them located at the 3′ neighboring linker region of the nucleosome to which it is bound, while the exposed region created by NF-1 is located next to it. Although the binding of the factors has a clear effect on restriction enzyme accessibility (Fig. 6B), only a small fraction of the templates shows these effects. We suggest that the small fraction of cleaved chromatin in the presence of H1 may be due to a short-lasting accessibility as a consequence of highly dynamic factor binding to compacted chromatin.

The addition of FoxE1 and NF-1 together had no effect on

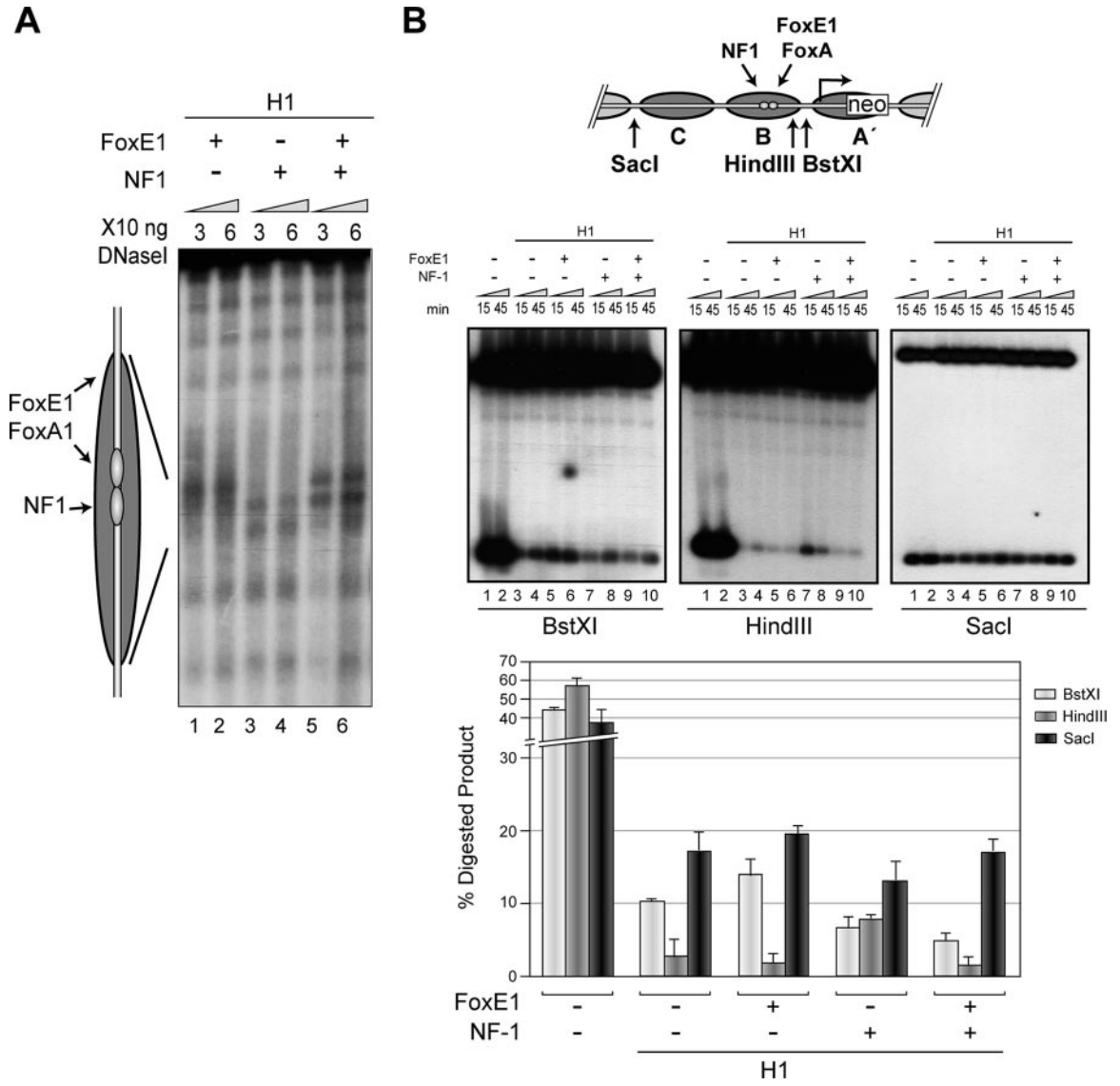

FIG. 6. Effect of FoxE1 and NF-1 on particle B in compacted nucleosome arrays. (A) Partial DNase I digestion of the H1-compacted TPO-5b nucleosome arrays incubated with FoxE1, NF-1, or both. On the left is a schematic representation indicating the positions of FoxE1 and NF-1 binding sites as lighter ellipses inside particle B. (B) Restriction enzyme accessibility assay of the arrays using three different enzymes. The drawing shows the nucleosome position over TPO promoter sequences inside the nucleosome arrays; the binding sites for FoxE1, FoxA1, and NF-1; and the cutting positions of BstXI, HindIII, and SacI. Below, representative gels are shown of digestions with the above-mentioned enzymes, with the uncut and cut products indicated. The panel shows quantification of the bands from the 45-min time point indicated as percentages of digested product with respect to undigested product. The values are the means and ranges of two separate experiments.

the accessibility of any of the restriction sites (Fig. 6B, lanes 9 and 10): the effects created by each of them alone on the specific restriction sequences disappeared. The possibility of a reciprocal sequestering mediated by an interaction between FoxE1 and NF-1 (39) can be ruled out, since both factors together have an additive effect on the DNase I hypersensitivity of TPO nucleosome arrays. On the other hand, if we consider the three-dimensional structure of nucleosome B, the observed effect could be the consequence of a possible proximity of the BstXI and HindIII restriction sites to the FoxE1 and NF-1 binding sites, where each factor would occlude the restriction site exposed by the other factor.

DISCUSSION

The transcription factor FoxE1 regulates the expression of the thyroid-specific TPO and Tg genes (2, 19) and of other genes yet to be characterized (23). The FoxE1 binding site constitutes an essential hormone response element of the TPO and Tg promoters, but until now very little was known about the molecular mechanism of its action, apart from a weak transcriptional activator activity (2, 40). In this study, we have shown that FoxE1 binding to the TPO promoter precedes its transcriptional activation and occurs simultaneously with the appearance of highly accessible regions in the chromatin struc-

ture of this promoter. By using an in vitro system, we also have demonstrated that FoxE1 binding to the TPO promoter by itself is sufficient to modify compacted chromatin structures, creating a locally exposed domain. This in vitro activity leads us to believe that the alteration of the in vivo promoter structure during its activation is provoked at least in part by the specific binding of FoxE1 to the inactive promoter conformation.

FoxE1 is a member of the Forkhead family of transcription factors, which play essential roles in differentiation, proliferation, and metabolism (1, 5, 26, 29). While the similarity of the DNA binding domain to linker histones has led many to propose that Forkhead factors in general regulate chromatin structure (5), to date there has been evidence for one only member, FoxA1, being able to bind and alter compacted chromatin structures (8). The present study shows that FoxE1 is also capable of initiating chromatin-opening events in a biologically relevant context, during thyroid differentiation, which substantially strengthens the hypothesis that Forkhead factors may generally regulate chromatin structure.

The TPO gene is thyroid specific, and its expression coincides with thyroid gland differentiation during development (15, 19, 37). Here we show that the chromatin structure of the native TPO promoter varies among different states of cell differentiation, indicating that it can constitute a decisive regulatory aspect of gene expression, as has been reported for many other tissue-specific genes (21). Thus, the TPO gene constitutes a model system to study the involvement of chromatin structure regulation in thyroid-specific gene expression during thyroid differentiation. We find that when FoxE1 starts to be expressed, it binds to the inactive TPO promoter, which precedes strong promoter activity and coincides with the appearance of nuclease hypersensitivity over particle B.

The in vitro simulation of the TPO promoter chromatin structure by use of nucleosome arrays has allowed the direct characterization of FoxE1 effects (49). FoxE1 overcomes the DNA accessibility restrictions imposed by H1 binding and creates an exposed domain in compacted chromatin in a local and specific manner that extends over the neighboring linker regions. This domain presents two DNase I-hypersensitive regions, at the FoxE1 binding site and near the 3′ end of the nucleosome, similar to those observed in vivo. FoxE1 binding also increased the accessibility of a restriction enzyme to its site located at the same nucleosome particle, although this effect is subtle—possibly as a consequence of a highly dynamic binding to compacted chromatin. The difference between this dynamic binding on the more stable compacted arrays and that seen for free DNA or noncompacted arrays could be due to parameters involved in array compaction that occlude the protein binding site.

The latter observation agrees with the weak in vivo hypersensitivity at the FoxE1 binding site at the initial state of activation (2 h of induction) compared to the footprints seen for the AC state (more than 24 h after induction). Thus, the chromatin structure alterations seen at the initial stages of TPO gene activation appear to be, at least in part, a consequence of FoxE1 binding.

NF-1 binds 10 bp upstream of the FoxE1 binding site to enhance the action of FoxE1 in the hormone-induced expression of the TPO gene (39), and the simultaneous binding of these factors has been demonstrated by in vitro footprinting with nuclear extracts from thyroid and nonthyroid cells (19, 39). The in vivo footprinting experiments presented here confirm the in vitro data, showing the same protection over FoxE1-NF-1 binding sites in vivo and in vitro; the ChIP assay corroborates that these two factors are indeed present at the promoter.

Previous studies have demonstrated that FoxE1 and NF-1 can interact physically, and the spatial orientation of both binding sites in the TPO promoter at the same side of the DNA helix is essential for maximum transcriptional activity and for the ability of the promoter to respond to the hormones (39). This cooperative role of NF-1 has been reported for other regulatory systems, such as the mouse mammary tumor virus promoter (16) and the albumin enhancer (25). It has therefore been proposed that the interaction between Forkhead factors and NF-1 could be a general mechanism of action of both transcription factor families (39). Unlike the other mentioned regulatory systems, NF-1 is able to alter the accessibility to its binding site localized over a positioned nucleosomal particle, in either extended or H1-compacted TPO-arrays, without the aid of an already bound factor. This main divergence between systems could be due to a difference in the position of the NF-1 binding site relative to the nucleosome surface, although there is no presented evidence for this. FoxE1 and NF-1 can alter the structure of H1-compacted nucleosome arrays in different manners, and when both are together they exert an additive effect.

But in vivo the situation is different, since although NF-1 is expressed in quiescent cells (39) in which the TPO gene is inactive (2), it exhibits minimal occupancy of the TPO promoter. Solely upon the induction of FoxE1, NF-1 was significantly engaged at the promoter. The different accessibilities of NF-1 to the compacted TPO promoters in vitro and in vivo may indicate the presence of other factors apart from H1 eliciting a more complex compacted chromatin structure, which would lead to an inaccessible structure for NF-1 but not for FoxE1; binding of this latter factor might alter the chromatin structure in a specific manner. Other scenarios, such as a different positioning of the NF-1 binding site over the TPO chromatin structure in vivo, are also feasible. Taking all known data into account, we propose a model according to which FoxE1 helps NF-1 load onto chromatin and, once bound, NF-1 enhances the accessibility of the TPO promoter to a level beyond that initiated by FoxE1 (Fig. 7). The FoxE1 unbound and bound states may be in a highly dynamic equilibrium, as represented in Fig. 7, causing an initial distortion of the compacted structure of the promoter that is sufficient to allow the binding of other factors that regulate TPO, which, like NF-1, are present at detectable levels in the noninduced cells but the occupancy of whose binding sites occurs only after FoxE1 binding. We therefore suggest that FoxE1, which is intrinsically a weak transcriptional activator by itself (2, 40), is a pioneer factor whose primary mechanistic role in mediating the hormonal response of TPO is to enable other factors to access the chromatin (Fig. 7). In our model, these changes in chromatin structure would bestow transcriptional competence on FoxE1-regulated genes during thyroid cell differentiation, thus expanding this functional characteristic to other members of the Forkhead transcription factor family.

In vivo, FoxA1 and FoxE1 also cause similar footprints over

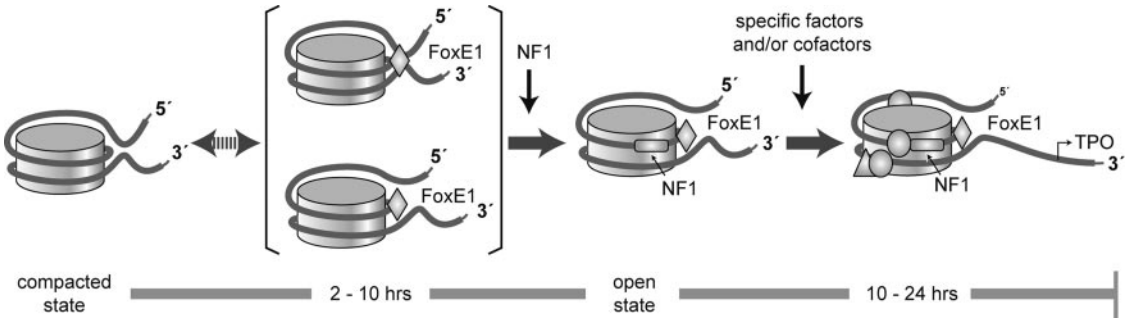

FIG. 7. Model of the sequential steps involved in the activation of TPO expression. The expression of FoxE1 is rapidly induced during thyroid cell differentiation and constitutes one of the first events in the activation of the thyroid-specific TPO gene. FoxE1 may bind initially to the compacted chromatin structure present at the inactive TPO promoter, generating an altered/open state of the regulatory particle that contains all the known transcription factor binding sites. NF-1, which is expressed in all the differentiation conditions, now can occupy its site over the altered particle, and both factors together further alter the structure of the regulatory particle, stabilizing the open state. This stable ternary complex is now a good platform for the binding of the other regulatory transcription factors and cofactors essential for TPO gene expression. The double-headed arrow indicates that the FoxE1 unbound and bound states may be in a highly dynamic equilibrium; brackets indicate an initial distortion of the compacted structure of the promoter.

their binding sites at the albumin enhancer (35) and the TPO promoter, respectively, a simultaneous enhancement and protection of guanines to methylation, and the well-known DNase I hypersensitivity. Also, the NF-1 site located next to the Fox site presents partial protection in both systems. This similarity extends to nucleosome array systems of each regulatory element, since both FoxA1 (8) and FoxE1 factors are able to bind and modify the structure of H1-compacted nucleosomes. Furthermore FoxA1, which can bind to the TPO promoter FoxE1 site (44), distorts the compacted chromatin structure of TPO arrays, creating the same DNase I hypersensitivity pattern as seen for FoxE1, although with higher intensity.

As FoxA1 is a pioneer factor that is already bound to the albumin enhancer in endoderm cells during liver development (4) prior to albumin expression, the molecular mechanism similarity between these two factors supports our model proposing a pioneer role for the FoxE1 factor, which is capable of initiating chromatin-opening events of the TPO promoter during hormonally induced differentiation. This hypothesis could be extended to a possible pioneer role of FoxE1 during development, since the stable expression of FoxE1 in kidney cells stimulates the expression of several genes with significant roles in thyroid development (23). Indeed, mutations in the FoxE1 gene cause severe thyroid defects in humans (3, 7, 11), and FoxE1 knockout mouse models show either a sublingual or a completely absent thyroid gland (14). The lack of a more drastic phenotype could be explained by a partial compensation by FoxA1 expressed in thyroid cells (44), which are endoderm derived. More-recent studies have reported a pioneer activity for another Forkhead family member, FoxI1, which binds condensed mitotic chromosomes and modulates chromatin structures (54).

By reporting the regulation of chromatin structure by FoxE1 during hormonally induced thyroid differentiation, the present study has contributed to the hypothesis of a general pioneer role for the Forkhead factors, one mediated by their ability to bind and alter chromatin structures during tissue specification and cell differentiation. Considering the increasing number of Forkhead factors known to play essential roles in these processes and the association of their deregulation and mutation with numerous human pathologies, such as congenital disorders, diabetes mellitus, and carcinogenesis (5, 7, 11, 26, 30, 33, 51), a deeper understanding of the molecular mechanism of chromatin structure modulation by Forkhead factors would be of considerable interest and should provide insights of general relevance.

ACKNOWLEDGMENTS

We thank Roberto Di Lauro (BIOGEM, Ariano Irpino, Avellino, Italy) for the FoxE1 antibody and Alfredo Fusco (Università degli Studi, Naples, Italy) for PCCl3 cells, Margarita González-Monge for technical support, Custodia Garcia-Jiménez for introducing us into the chromatin field, and Ronald Hartong for his criticisms and his linguistic assistance.

I.C. was awarded the 2004 Salvatore-BRAHMS-Young Investigator Award and the Juan March prize of the "Epigenetics and Chromatin: Transcriptional Regulation and Beyond" workshop 2005. The research was supported by a FIS-Instituto de Salud Carlos III predoctoral grant (BEFI 99/9143) to I.C.; BFU2004-03169 from the Ministerio de Educación y Ciencia and FIS-ISCIII (RD06/0020/0060), PI042374, and PI041216 grants to P.S.; NIH (GM47903) and Mathers Charitable Foundation grants to K.S.Z.; and a U.S.-Spain Fulbright award to P.S. and K.S.Z.

REFERENCES

1. **Accili, D., and K. C. Arden.** 2004. FoxOs at the crossroads of cellular metabolism, differentiation, and transformation. Cell **117:**421–426.
2. **Aza-Blanc, P., R. Di Lauro, and P. Santisteban.** 1993. Identification of a cis-regulatory element and a thyroid-specific nuclear factor mediating the hormonal regulation of rat thyroid peroxidase promoter activity. Mol. Endocrinol. **7:**1297–1306.
3. **Baris, I., A. E. Arisoy, A. Smith, M. Agostini, C. S. Mitchell, S. M. Park, A. M. Halefoglu, E. Zengin, V. K. Chatterjee, and E. Battaloglu.** 2006. A novel missense mutation in human TTF-2 (FKHL15) gene associated with congenital hypothyroidism but not athyreosis. J. Clin. Endocrinol. Metab. **91:**4183–4187. [Epub ahead of print.]
4. **Bossard, P., and K. S. Zaret.** 1998. GATA transcription factors as potentiators of gut endoderm differentiation. Development **125:**4909–4917.
5. **Carlsson, P., and M. Mahlapuu.** 2002. Forkhead transcription factors: key players in development and metabolism. Dev. Biol. **250:**1–23.
6. **Carroll, J. S., X. S. Liu, A. S. Brodsky, W. Li, C. A. Meyer, A. J. Szary, J. Eeckhoute, W. Shao, E. V. Hestermann, T. R. Geistlinger, E. A. Fox, P. A. Silver, and M. Brown.** 2005. Chromosome-wide mapping of estrogen receptor binding reveals long-range regulation requiring the forkhead protein FoxA1. Cell **122:**33–43.
7. **Castanet, M., S. M. Park, A. Smith, M. Bost, J. Leger, S. Lyonnet, A. Pelet, P. Czernichow, K. Chatterjee, and M. Polak.** 2002. A novel loss-of-function mutation in TTF-2 is associated with congenital hypothyroidism, thyroid agenesis and cleft palate. Hum. Mol. Genet. **11:**2051–2059.

8. **Cirillo, L. A., F. R. Lin, I. Cuesta, D. Friedman, M. Jarnik, and K. S. Zaret.** 2002. Opening of compacted chromatin by early developmental transcription factors HNF3 (FoxA) and GATA-4. Mol. Cell **9:**279–289.
9. **Cirillo, L. A., C. E. McPherson, P. Bossard, K. Stevens, S. Cherian, E. Y. Shim, K. L. Clark, S. K. Burley, and K. S. Zaret.** 1998. Binding of the winged-helix transcription factor HNF3 to a linker histone site on the nucleosome. EMBO J. **17:**244–254.
10. **Clark, K. L., E. D. Halay, E. Lai, and S. K. Burley.** 1993. Co-crystal structure of the HNF-3/fork head DNA-recognition motif resembles histone H5. Nature **364:**412–420.
11. **Clifton-Bligh, R. J., J. M. Wentworth, P. Heinz, M. S. Crisp, R. John, J. H. Lazarus, M. Ludgate, and V. K. Chatterjee.** 1998. Mutation of the gene encoding human TTF-2 associated with thyroid agenesis, cleft palate and choanal atresia. Nat. Genet. **19:**399–401.
12. **Dathan, N., R. Parlato, A. Rosica, M. De Felice, and R. Di Lauro.** 2002. Distribution of the titf2/foxe1 gene product is consistent with an important role in the development of foregut endoderm, palate, and hair. Dev. Dyn. **224:**450–456.
13. **De Felice, M., and R. Di Lauro.** 2004. Thyroid development and its disorders: genetics and molecular mechanisms. Endocr. Rev. **25:**722–746.
14. **De Felice, M., C. Ovitt, E. Biffali, A. Rodriguez-Mallon, C. Arra, K. Anastassiadis, P. E. Macchia, M. G. Mattei, A. Mariano, H. Scholer, V. Macchia, and R. Di Lauro.** 1998. A mouse model for hereditary thyroid dysgenesis and cleft palate. Nat. Genet. **19:**395–398.
15. **De Felice, M., M. P. Postiglione, and R. Di Lauro.** 2004. Thyrotropin receptor signaling in development and differentiation of the thyroid gland: insights from mouse models and human diseases. Endocrinology **145:**4062–4067.
16. **Di Croce, L., R. Koop, P. Venditti, H. M. Westphal, K. P. Nightingale, D. F. Corona, P. B. Becker, and M. Beato.** 1999. Two-step synergism between the progesterone receptor and the DNA-binding domain of nuclear factor 1 on MMTV minichromosomes. Mol. Cell **4:**45–54.
17. **Eissenberg, J. C.** 2001. Decisive factors: a transcription activator can overcome heterochromatin silencing. Bioessays **23:**767–771.
18. **Fournier, C., Y. Goto, E. Ballestar, K. Delaval, A. M. Hever, M. Esteller, and R. Feil.** 2002. Allele-specific histone lysine methylation marks regulatory regions at imprinted mouse genes. EMBO J. **21:**6560–6570.
19. **Francis-Lang, H., M. Price, M. Polycarpou-Schwarz, and R. Di Lauro.** 1992. Cell-type-specific expression of the rat thyroperoxidase promoter indicates common mechanisms for thyroid-specific gene expression. Mol. Cell. Biol. **12:**576–588.
20. **Fusco, A., M. T. Berlingieri, P. P. Di Fiore, G. Portella, M. Grieco, and G. Vecchio.** 1987. One- and two-step transformations of rat thyroid epithelial cells by retroviral oncogenes. Mol. Cell. Biol. **7:**3365–3370.
21. **Gilbert, N., S. Boyle, H. Fiegler, K. Woodfine, N. P. Carter, and W. A. Bickmore.** 2004. Chromatin architecture of the human genome: gene-rich domains are enriched in open chromatin fibers. Cell **118:**555–566.
22. **Gualdi, R., P. Bossard, M. Zheng, Y. Hamada, J. R. Coleman, and K. S. Zaret.** 1996. Hepatic specification of the gut endoderm in vitro: cell signaling and transcriptional control. Genes Dev. **10:**1670–1682.
23. **Hishinuma, A., N. Ohmika, T. Namatame, and T. Ieiri.** 2004. TTF-2 stimulates expression of 17 genes, including one novel thyroid-specific gene which might be involved in thyroid development. Mol. Cell. Endocrinol. **221:**33–46.
24. **Horn, P. J., and C. L. Peterson.** 2002. Chromatin higher order folding—wrapping up transcription. Science **297:**1824–1827.
25. **Jackson, D. A., K. E. Rowader, K. Stevens, C. Jiang, P. Milos, and K. S. Zaret.** 1993. Modulation of liver-specific transcription by interactions between hepatocyte nuclear factor 3 and nuclear factor 1 binding DNA in close apposition. Mol. Cell. Biol. **13:**2401–2410.
26. **Katoh, M.** 2004. Human FOX gene family. Int. J. Oncol. **25:**1495–1500.
27. **Khorasanizadeh, S.** 2004. The nucleosome: from genomic organization to genomic regulation. Cell **116:**259–272.
28. **Kitagawa, H., R. Fujiki, K. Yoshimura, Y. Mezaki, Y. Uematsu, D. Matsui, S. Ogawa, K. Unno, M. Okubo, A. Tokita, T. Nakagawa, T. Ito, Y. Ishimi, H. Nagasawa, T. Matsumoto, J. Yanagisawa, and S. Kato.** 2003. The chromatin-remodeling complex WINAC targets a nuclear receptor to promoters and is impaired in Williams syndrome. Cell **113:**905–917.
29. **Lee, C. S., J. R. Friedman, J. T. Fulmer, and K. H. Kaestner.** 2005. The initiation of liver development is dependent on Foxa transcription factors. Nature **435:**944–947.
30. **Lehmann, O. J., J. C. Sowden, P. Carlsson, T. Jordan, and S. S. Bhattacharya.** 2003. Fox's in development and disease. Trends Genet. **19:**339–344.
31. **Lu, Q., and B. Richardson.** 2004. DNaseI hypersensitivity analysis of chromatin structure. Methods Mol. Biol. **287:**77–86.
32. **Maier, H., R. Ostraat, H. Gao, S. Fields, S. A. Shinton, K. L. Medina, T. Ikawa, C. Murre, H. Singh, R. R. Hardy, and J. Hagman.** 2004. Early B cell factor cooperates with Runx1 and mediates epigenetic changes associated with mb-1 transcription. Nat. Immunol. **5:**1069–1077.
33. **Marson, A., K. Kretschmer, G. M. Frampton, E. S. Jacobsen, J. K. Polansky, K. D. MacIsaac, S. S. Levine, E. Fraenkel, H. von Boehmer, and R. A. Young.** 2007. Foxp3 occupancy and regulation of key target genes during T-cell stimulation. Nature **445:**931–935.
34. **Maxam, A. M., and W. Gilbert.** 1977. A new method for sequencing DNA. Proc. Natl. Acad. Sci. USA **74:**560–564.
35. **McPherson, C. E., E. Y. Shim, D. S. Friedman, and K. S. Zaret.** 1993. An active tissue-specific enhancer and bound transcription factors existing in a precisely positioned nucleosomal array. Cell **75:**387–398.
36. **Mellor, J.** 2005. The dynamics of chromatin remodeling at promoters. Mol. Cell **19:**147–157.
37. **Missero, C., G. Cobellis, M. De Felice, and R. Di Lauro.** 1998. Molecular events involved in differentiation of thyroid follicular cells. Mol. Cell. Endocrinol. **140:**37–43.
38. **Mueller, P. R., and B. Wold.** 1989. In vivo footprinting of a muscle specific enhancer by ligation mediated PCR. Science **246:**780–786.
39. **Ortiz, L., P. Aza-Blanc, M. Zannini, A. C. Cato, and P. Santisteban.** 1999. The interaction between the forkhead thyroid transcription factor TTF-2 and the constitutive factor CTF/NF-1 is required for efficient hormonal regulation of the thyroperoxidase gene transcription. J. Biol. Chem. **274:**15213–15221.
40. **Ortiz, L., M. Zannini, R. Di Lauro, and P. Santisteban.** 1997. Transcriptional control of the forkhead thyroid transcription factor TTF-2 by thyrotropin, insulin, and insulin-like growth factor I. J. Biol. Chem. **272:**23334–23339.
41. **Parlato, R., A. Rosica, A. Rodriguez-Mallon, A. Affuso, M. P. Postiglione, C. Arra, A. Mansouri, S. Kimura, R. Di Lauro, and M. De Felice.** 2004. An integrated regulatory network controlling survival and migration in thyroid organogenesis. Dev. Biol. **276:**464–475.
42. **Ramakrishnan, V., J. T. Finch, V. Graziano, P. L. Lee, and R. M. Sweet.** 1993. Crystal structure of globular domain of histone H5 and its implications for nucleosome binding. Nature **362:**219–223.
43. **Santisteban, P., A. Acebron, M. Polycarpou-Schwarz, and R. Di Lauro.** 1992. Insulin and insulin-like growth factor I regulate a thyroid-specific nuclear protein that binds to the thyroglobulin promoter. Mol. Endocrinol. **6:**1310–1317.
44. **Sato, K., and R. Di Lauro.** 1996. Hepatocyte nuclear factor 3beta participates in the transcriptional regulation of the thyroperoxidase promoter. Biochem. Biophys. Res. Commun. **220:**86–93.
45. **Simpson, R. T., F. Thoma, and J. M. Brubaker.** 1985. Chromatin reconstituted from tandemly repeated cloned DNA fragments and core histones: a model system for study of higher order structure. Cell **42:**799–808.
46. **Sinclair, A. J., R. Lonigro, D. Civitareale, L. Ghibelli, and R. Di Lauro.** 1990. The tissue-specific expression of the thyroglobulin gene requires interaction between thyroid specific and ubiquitous factors. Eur. J. Biochem. **193:**311–318.
47. **Soutoglou, E., and I. Talianidis.** 2002. Coordination of PIC assembly and chromatin remodeling during differentiation-induced gene activation. Science **295:**1901–1904.
48. **Spangenberg, C., K. Eisfeld, W. Stunkel, K. Luger, A. Flaus, T. J. Richmond, M. Truss, and M. Beato.** 1998. The mouse mammary tumour virus promoter positioned on a tetramer of histones H3 and H4 binds nuclear factor 1 and OTF1. J. Mol. Biol. **278:**725–739.
49. **Steger, D. J., T. Owen-Hughes, S. John, and J. L. Workman.** 1997. Analysis of transcription factor-mediated remodeling of nucleosomal arrays in a purified system. Methods **12:**276–285.
50. **Steger, D. J., and J. L. Workman.** 1997. Stable co-occupancy of transcription factors and histones at the HIV-1 enhancer. EMBO J. **16:**2463–2472.
51. **Uhlenhaut, N. H., and M. Treier.** 2006. Foxl2 function in ovarian development. Mol. Genet. Metab. **88:**225–234.
52. **Wolffe, A. P.** 1997. Histone H1. Int. J. Biochem. Cell Biol. **29:**1463–1466.
53. **Workman, J. L., and R. E. Kingston.** 1998. Alteration of nucleosome structure as a mechanism of transcriptional regulation. Annu. Rev. Biochem. **67:**545–579.
54. **Yan, J., L. Xu, G. Crawford, Z. Wang, and S. M. Burgess.** 2006. The forkhead transcription factor FoxI1 remains bound to condensed mitotic chromosomes and stably remodels chromatin structure. Mol. Cell. Biol. **26:**155–168.
55. **Zannini, M., V. Avantaggiato, E. Biffali, M. I. Arnone, K. Sato, M. Pischetola, B. A. Taylor, S. J. Phillips, A. Simeone, and R. Di Lauro.** 1997. TTF-2, a new forkhead protein, shows a temporal expression in the developing thyroid which is consistent with a role in controlling the onset of differentiation. EMBO J. **16:**3185–3197.
56. **Zaret, K.** 1999. Developmental competence of the gut endoderm: genetic potentiation by GATA and HNF3/fork head proteins. Dev. Biol. **209:**1–10.
57. **Zaret, K. S., and K. Stevens.** 1995. Expression of a highly unstable and insoluble transcription factor in Escherichia coli: purification and characterization of the fork head homolog HNF3 alpha. Protein Expr. Purif. **6:**821–825.
58. **Zarrilli, R., S. Formisano, and B. Di Jeso.** 1990. Hormonal regulation of thyroid peroxidase in normal and transformed rat thyroid cells. Mol. Endocrinol. **4:**39–45.